FORMATION OF CORONAL SHOCK WAVES

[1]Slaven Lulić, [2]Tomislav Žic, [2]Bojan Vršnak

[1] Karlovac University of Applied Sciences, Trg J.J. Strossmayera 9, HR-47000 Karlovac, Croatia

[2] Hvar Observatory, Faculty of Geodesy, University of Zagreb, Kačićeva 26, HR-10000 Zagreb, Croatia

e-mail: slulic@vuka.hr, tzic@geof.hr, bvrsnak@geof.hr

INTRODUCTION

Numerical simulations of magnetosonic wave formation driven by an expanding cylindrical piston are performed to get better physical insight into the initiation and evolution of large-scale coronal waves caused by coronal eruptions. Several very basic initial configurations are employed to analyze intrinsic characteristics of the MHD wave formation that do not depend on specific properties of the environment. It turns out that these simple initial configurations result in piston/wave morphologies and kinematics that reproduce common characteristics of coronal waves. In the initial stage the wave and the expanding source-region cannot be clearly resolved, i.e. a certain time is needed before the wave detaches from the piston. Thereafter, it continues to travel as a so-called "simple wave".

During the acceleration stage of the source-region inflation, the wave is driven by the piston expansion, so its amplitude and phase-speed increase, whereas the wavefront profile steepens.

MODEL

We consider perpendicular magnetosonic waves, where we focus on a planar and cylindrical geometry. This allows us to set the magnetic field in the z-direction, whereas the x and y magnetic-field components, as well as the z-component of the velocity, are always kept zero ($B_x=0$, $B_y=0$, $v_z=0$). Furthermore, all quantities are invariant along the z-coordinate, i.e. we perform 2.5D simulations, where the input and the basic output quantities are the density ρ the momentum $m_x=\rho v_x$, $m_y=\rho v_y$ and the magnetic field B_z. We use a two-dimensional [2D] numerical mesh containing 995x995 cells, supplemented by two ghost-cell layers at each boundary, which are used to regulate the boundary conditions (thus, the complete grid consists of 999x999 cells). All quantities are normalized, so that distances are expressed in units of the numerical-box length (L=1), velocities are normalized to the Alfvén speed v_A, and time is expressed in terms of the Alfvén travel time over the numerical-box length ($t_A=L/v_A$). We apply the approximation β=0, where β is the plasma-to-magnetic pressure ratio. The origin of the coordinate system is set at the numerical-box center.Widening the source is driven by a gradient of the magnetic pressure, setting the "parabolic" profile of the magnetic field within the area of origin.

$$B_z(x)=\sqrt{B_0^{\,2}-b_x^{\,2}}$$

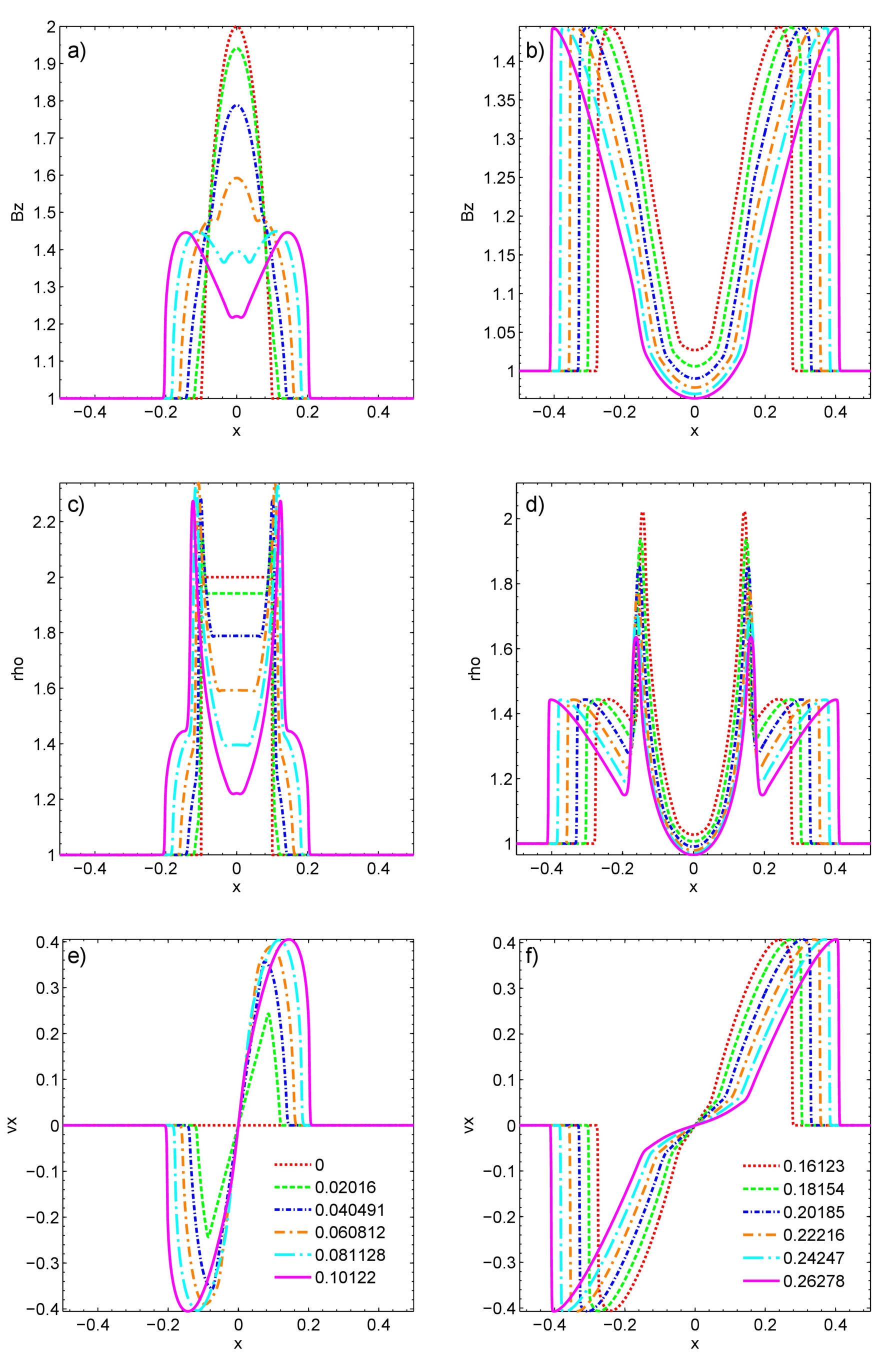

Figure 1

The formation and expansion of the wave is presented in Figure 1. In figures 1a and 1b, the spatial profiles of the magnetic field $B_z(x)$, in figures 1c and 1d density profiles ρ(x), and in figs 1e and 1f flow rate $v_x(x)$. Graphs on the left shows the phase of forming the wave, while those on the right side represent phase expansion.

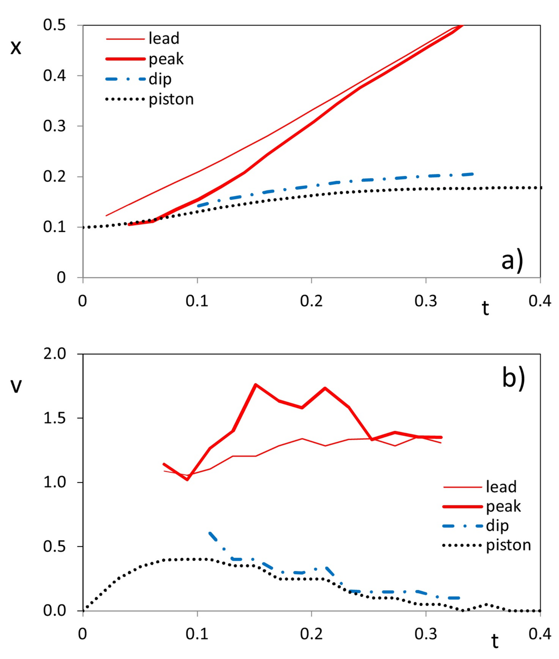

Figure 2

Figure 2 shows the edge of the wave fronts, maximum wave slope between the wave and the piston, and the border areas of origin. Most piston acceleration occurs to t≈0.08. It continues with the movement of a constant speed of approximately v≈0.4 to t≈0.13. During this period, the amplitude of the wave is growing, and the phase velocity of the wave crest rises w≈1 to w=1.76. The leading edge of the wavefront moving from w≈1. Top wave reaches the leading edge at t≈0.25 (the formation of the shock wave is completed), after which the front shock wave moving at a speed of w=1.35, which is in line with the Rankine-Hugoniot relations. The evolution of source / wave systems and related cinematics are fully consistent with the analytical model (w = 1 + 3v / 2) presented by Vršnak and Lulić(2000a).

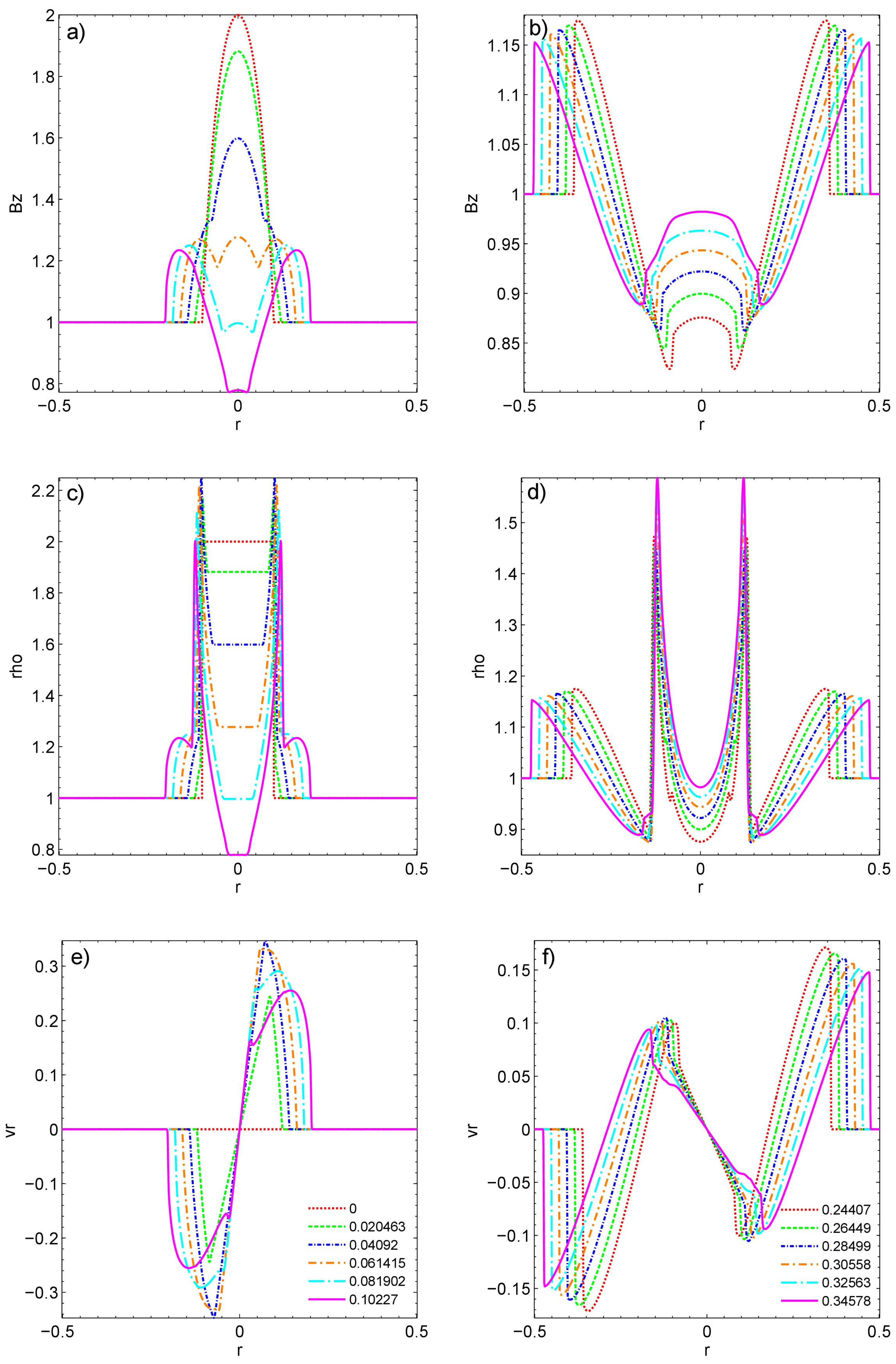

$$B_z(r)=B_0\cos^2\left(\frac{\pi}{2}\frac{r}{r_0}\right)+B_e$$

Figure 3

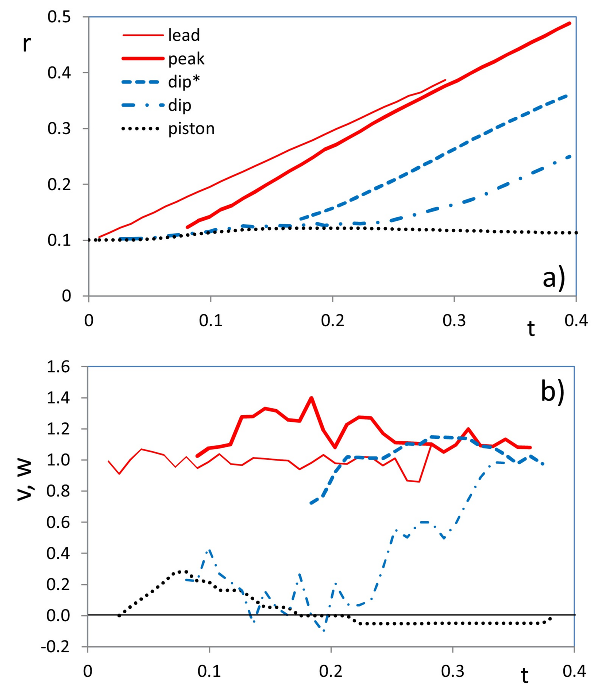

Figure 4

Figure 3 shows the creation and spreading of the wave in the cylindrical geometry. The spatial profile of the magnetic field Bz(r), as shown in Figures 3a and b, the density profile ρ(r), in Figures 3c and d, while in Figures 3e and f shown in the flow velocity $v_r(r)$. Acceleration phase is shorter than in the case of flat geometry, the maximum speed is much lower, and the missing phase v≈const. Once it reaches maximum speed, the piston is gradually slowing down and stops. Figure 4 shows the phase velocity of the wave maximum ascending from w≈1 to w≈1.3 for t≥0.15, and thereafter, gradually decreases. The slope between the band maximum and the piston, which is formed around t≈0.08, initially closely follows the kinematics of the piston, but then, after the slope becomes characterized with ρ <1 in t≈0.2, "discharged" from the piston and reaches a top speed of w≈1 about t≈0.35.

CONCLUSION

Common for all the analyzed situations, is that the expansion of the field of impulsive sources results in a shorter time/distance required for the formation of the shock wave, which is consistent with the analytical considerations. Simulations show that in most cases impulsive shock wave is formed very close to the border areas of source so it is initially difficult to separate the two entities.

However, for large amplitude numerical results differ from the analytical theory, most likely due to the numerical resolution. From the observation point of view, the cylindrical geometry is much more interesting, because it provides insight into the process of creating a shock wave driven by the expansion of the magnetic arcades, and includes an amplitude reduction due to energy conservation (Žic et al., 2008).

Our next step will be performing similar simulations, but using real initial configurations that include chromosphere, transition-region and corona.

Acknowledgments

We acknowledge the support of European Social Fund under the „PoKRet“ project.